energies

MDPI

Article

Robust Distributed Secondary Voltage Restoration Control of AC Microgrids under Multiple Communication Delays

Milad Gholami, Alessandro Pilloni *, Alessandro Pisano and Elio Usai

Department of Electrical and Electronic Engineering (DIEE), University of Cagliari, 09123 Cagliari, Italy; milad.gholami@unica.it (M.G.); apisano@unica.it (A.P.); elio.usai@unica.it (E.U.)
* Correspondence: alessandro.pilloni@unica.it; Tel.: +39-070-6755768

Abstract: This paper focuses on the robust distributed secondary voltage restoration control of AC microgrids (MGs) under multiple communication delays and nonlinear model uncertainties. The problem is addressed in a multi-agent fashion where the generators' local controllers play the role of cooperative agents communicating over a network and where electrical couplings among generators are interpreted as disturbances to be rejected. Communications are considered to be affected by heterogeneous network-induced time-varying delays with given upper-bounds and the MG is subjected to nonlinear model uncertainties and abrupt changes in the operating working condition. Robustness against uncertainties is achieved by means of an integral sliding mode control term embedded in the control protocol. Then, the global voltage restoration stability, despite the communication delays, is demonstrated through a Lyapunov-Krasovskii analysis. Given the delays' bounds, and because the resulting stability conditions result in being non-convex with respect to the controller gain, then a relaxed linear matrix inequalities-based tuning criteria is developed to maximize the controller tuning, thus minimizing the restoration settling-time. By means of that, a criteria to estimate the maximal delay margin tolerated by the system is also provided. Finally, simulations on a faithful nonlinear MG model, showing the effectiveness of the proposed control strategy, are further discussed.

Keywords: microgrid; voltage control; multi-agent systems; secondary control; sliding mode control; time delay systems; consensus algorithms; linear matrix inequalities

Citation: Gholami, M.; Pilloni, A.; Pisano, A.; Usai, E. Robust Distributed Secondary Voltage Restoration Control of AC Microgrids under Multiple Communication Delays. *Energies* **2021**, *14*, 1165. https://doi.org/10.3390/en14041165

Academic Editors: Amedeo Andreotti and Alberto Petrillo

Received: 22 December 2020
Accepted: 16 February 2021
Published: 22 February 2021

1. Introduction

Microgrids (MGs) are small-scale power systems consisting of localized grouping of Distributed Generators (DGs), storage systems and loads. In general, MGs operate either in islanded, autonomous mode or connected to the main power system. Recently the MG control system has been standardized into three layers [1]. The inner layer is called "Primary Control". It generates the actual command for the DG power converters' DC-AC interfaces. Commonly, it is implemented in a decentralized way and consists of the droop power control terms which aim to establish a desired power sharing among DGs and the inner voltage and current control loops. The "Secondary Control" layer enables the compensation of the frequency and voltage deviations introduced by the droop power control terms. This is because inverter-based DGs have no inertia [2]. Lastly, to optimize the DGs injected power from/to the main grid, a "Tertiary Control" layer is further designed. It allows us to adapt online the droop coefficients accordingly with the energy costs and the demand constraints imposed by the energy provider and vendors. It is worth mentioning that, among the three control layers, the secondary one is that of more practical interest to make compliant the integration of renewable resources within the AC power transmission paradigm. Moreover, due to the possibility of temporarily modifying the DGs' frequencies and output voltages to certain set-points while preserving the power sharing it would also be useful to perform the seamless and safe transition of the MG from islanded to the

grid-connected mode and vice-versa [3]. In particular this paper focuses on the design of a model-free robust multi-agent oriented secondary controller to guarantee the exact voltage restoration despite model uncertainties, unbalanced load variations, abrupt unplanned events and the effect of time-varying network-induced communications delays.

1.1. Literature Review

Earlier secondary control algorithms were centralized [1,4]. These solutions are now discouraged in favour of distributed approaches because they scale better with the MG size, are more robust to failures, and dispense with costly central computing and communication units [5]. Pioneer distributed controllers were based on Proportional-Integral (PI) schemes and assume the secondary control set-points globally available to all the DGs, see [6,7]. As an example, in [7] a Distributed Averaging PI control, combined with quadratic voltage feedbacks and feed-forward power terms is proposed to achieve voltage restoration under the additional reactive power sharing constraint among DGs. There, it is shown that only a compromise between the reactive power sharing accuracy and the voltage regulation precision can be achieved. On the other hand, since to reduce losses the reactive power flowing in the MG needs to be kept a close to zero as possible, then such an additional constraint is often not considered during the voltage control design. Despite this, and because the DG dynamics are strongly non-linear and coupled with each other, these strategies allow us to conclude stability properties only in the local sense. Thus, particular effort has been spent on designing robust strategies that aim to achieve the control objectives despite the presence of non-linearities and model uncertainties (see [6,8–10]). These investigations show that, to achieve the exact voltage restoration, the DG models must be perfectly known to properly design ad-hoc feedback linearization terms. These works further remove the requirement of globally available set-points, thus increasing the system flexibility while minimizing communications and global variables. Indeed, now the secondary control set-points are known only to a few DGs, referred to as "leader(s)". This enables the service provider to integrate higher level control strategies and ancillary services in the system through only local interaction. Compared with [7], and thanks to the perfect MG model knowledge, these works are enabled to guarantee global stability features; namely, in the large sense. Let us further note that among References [6,8–10], the proposal in [8] is superior since it guarantees the finite-time convergence property. However, since MGs consist of complex systems subjected to disturbances, uncertainties and changes in the operating conditions, the assumption of a perfect knowledge of the DG models is quite unrealistic in practice. Thus, aiming to introduce the concept of robustness in the secondary control layer design, ref. [11] proposed a model-free continuous voltage sliding-mode control (SMC) protocol that, under certain boundedness assumptions on the injected power by the DGs, globally solve the secondary control objective in finite-time as well. Finally, it is also worth mentioning [12] where the robust voltage restoration problem has been studied in the discrete-time setting, and [13], which adopts active disturbance rejection control technique combined with extended state observers to compensate model uncertainties and unknown perturbations.

Although all the mentioned strategies require a communication infrastructure, network induced delays that may degrade the MG performance, and even destabilize it, have been ignored. The impact of a constant identical delay for all the communications within the secondary control layer, that is, $\tau_{ij} = \tau$, is analysed first by [14], where i and j denote that DG j communicates with DG i. A step beyond is [15], where under the assumption that each communication from DG i to j yields $\tau_{ij}(t) = \tau_i(t)$ for all j; a multi-agent voltage control protocol accounting either averaging, and power compensation terms is proposed. Therein, sufficient conditions on the delay bounds that guarantee that the voltages will stay within a given boundary layer depending on the reactive power sharing accuracy is also provided. It is also worth mentioning the voltage secondary controllers proposed in [16–18], which assume, resp., a single constant and multiple constant delays per link. More realistic heterogeneous time-varying delays, such that $\tau_{ij}(t)$ is different for each pair

(i, j), are recounted in [19]. Therein, under the assumption of Markovian distributed delays and globally known set-points, a new stochastic small-signal MG model and a secondary controller is proposed. Small-signal analysis of an MG equipped with a time-delayed secondary voltage control is also studied in [20]. Therein, an analytical formula is developed to determine the individual delay margin for each link with respect to different sets of controller gains and leader pinning conditions. Lastly, we further mention [21], which proposes a time-delay tolerant distributed observer to track the average voltage of all DGs. Then, thanks to this estimation the implementation of lower level decentralized restoration strategies is enabled. Notice now that, although all the previously mentioned works account for the presence of different types of delays, all consist of a linear control protocol, thus they suffer the same limit of [7]. Indeed, they can only provide stability features in a local sense since their results are obtained by means of small signal analysis. Moreover, since they are linear, they cannot also face-off the presence of model non-linearities and/or disturbances.

Summarizing from the previous discussion it can be concluded that the control protocols that account robustness features against model uncertainties and disturbances are not able to face-off communication delays, whereas those designed to deal with the presence of communication delays lack robust control features because they are usually control protocols. Moreover, among the delay-oriented strategies, only [20] proposes a criterion for the secondary control tuning, whereas the other limits their analysis to provide necessary conditions for the closed loop stability within a local domain.

1.2. Statement of Contributions

Thus motivated, this paper proposes a robust voltage secondary control strategy that is able to perform the exact distributed tracking of the voltage set-point despite the absence of feedback-linearisation terms, and the presence of heterogeneous network-induced time-varying delays. Let us further note that the proposed control protocol is integral with discontinuous derivative thus well-suited to fed the inner control layers. It consists of two terms: (1) a distributed Integral SMC [22] component that aims to enforce each agent (DG) to behave as a reference unperturbed dynamic; (2) an ad-hoc designed distributed averaging control term aiming to globally, exponentially, achieve voltage restoration despite the non-uniform time-varying communication delays. A Lyapunov-Krasovskii analysis that used the simpler averaging problems, without [23], and with leaders [24], is also provided, and an LMI tuning criterion is established. Differently to the State-of-the-Art: (a) at the same time, both robust control concepts and the presence of multiple non-uniform time-varying communication delays are considered; (b) under the assumption that the power flowing within the MG is bounded, conditions for the robust global exponential stability of the system are established; (c) a new stability analysis for the MG's secondary control problem is proposed; (d) an off-line LMI-based algorithm aimed to find the maximal controller gain that, under the given delays bounds, guarantees the control objective is given along with criteria to estimate the corresponding maximal tolerated delay margin; (e) the robustification method in [22] is extended to the presence of delays among the agents' communications. Preliminary results of this research have been presented in [25]. However, although the controller structure here proposed is the same as in [25], this paper differs from that in the following aspects:

- Here a much more faithful MG modelization expressed in the *d*-*q*-reference frame is considered, whereas in our past work DGs were simply modelled as second-order coupled oscillators.
- The tuning criteria in our past work involves non-convex optimization which can thus hardly be solved in practice. On the other hand, our novel Algorithm 1 is based on the solution of a standard LMI problem, solvable by means of standard interior-point solvers.
- Here Lemma 1 proofs that matrix Φ in Algorithm 1 is always negative definite, whereas in our past work this was an operating assumption;

- The proposed control protocol is now tested on a realistic MG model which accounts, along with time-varying delays, 3-phase PWM controlled power bridges, noisy measurements with a realistic Signal-to-Noise Ratio, and unplanned faults.

Algorithm 1 Tuning algorithm for k in (35).

• **Initialize** the control gains $k = \bar{k}$ with $\bar{k} > 0$.
• **Define** the gain decrement $0 < \Delta k \ll \bar{k}$, the edges weight α_{ij} of $\mathcal{G}_{N+1}(0 \cup \mathcal{V}, \mathcal{E}_{N+1})$, the delay bounds $\tau_l^\star > 0$, $\sigma_g^\star > 0$, $\delta_l < 1$, $\delta_g < 1$, $\bar{B} = B \cdot [1, 2]$
• **Repeat until** $k > 0$
(a) Determine $\forall\, l$ and g the matrices $A_l(k) = [A_{l(r,y)}(k)]$, $\hat{A}_g(k) = [\hat{A}_{g(r,y)}(k)] \in \mathbb{R}^{2N \times 2N}$ where

$$\begin{aligned} A_{l(r,r)}(k) \quad &: \begin{cases} -\alpha_{i0} k \bar{B} & \text{if } \tau_l = \tau_{il},\ r = l = i \\ 0_{2\times 2} & \text{otherwise} \end{cases}, \\ \hat{A}_{g(r,y)}(k) \quad &: \begin{cases} -\alpha_{ij} k \bar{B} & \text{if } \sigma_g = \tau_{ij},\ i \neq j,\ r = y = i \\ \alpha_{ij} k \bar{B} & \text{if } \sigma_g = \tau_{ij},\ i \neq j,\ r = i,\ y = j \\ 0_{2\times 2} & \text{otherwise} \end{cases}, \end{aligned} \tag{1}$$

and the negative definite matrix $\Phi(k) \prec 0$

$$\Phi(k) = A_0 + \sum_{l=1}^{q} A_l(k) + \sum_{g=1}^{m} \hat{A}_g(k) \prec 0 \quad , \quad \forall\, k > 0 \quad \text{with} \quad A_0 = I_N \otimes A \tag{2}$$

(b) Solve for $\eta > 0$ and the positive definite matrices P, Q_l, Q_g, R_g, W_l, $W_g \in \mathbb{R}^{2N \times 2N}$ the LMI problem

$$P\Phi^\intercal(k) + P\Phi(k) \prec -\left(\sum_{l=1}^{q} Q_l + \sum_{g=1}^{m} Q_g + \sum_{g=1}^{m} \sigma_g^\star R_g \right) \tag{3}$$

$$-\sum_{g=1}^{m} \sigma_g^\star R_g \prec -\eta \cdot A_0^\intercal \left(\sum_{g=1}^{m} \sigma_g^\star W_g + \sum_{l=1}^{q} \tau_l^\star W_l \right) A_0 \tag{4}$$

$$-(1 - d_l) Q_l \prec -\eta \cdot A_l^\intercal(k) \left(\sum_{g=1}^{m} \sigma_g^\star W_g + \sum_{l=1}^{q} \tau_l^\star W_l \right) A_l(k) \tag{5}$$

$$-(1 - d_g) Q_g \prec -\eta \cdot \hat{A}_g^\intercal(k) \left(\sum_{g=1}^{m} \sigma_g^\star W_g + \sum_{l=1}^{q} \tau_l^\star W_l \right) \hat{A}_g(k) \tag{6}$$

(c) If the given solution satisfies (3) **then: Break**
Else: $k = k - \Delta k$ **EndIf**.

1.3. Paper Organization

This manuscript is organized as follows—in Section 2 the nonlinear modelization of a MG for secondary control purposes is given. The voltage secondary control problem, along with the proposed robust control strategy and the main paper results are illustrated in Section 3. In Section 4, the robustness of the proposed controller is confirmed by means of simulations on a faithful 3-phase nonlinear MG model accounting IGBT power-converters, time-varying communication delays, noisy measurements and uncertainties, and unplanned faults. Lastly, in Section 5, concluding remarks and possible hints for future research are provided.

1.4. Mathematical Notation

The set of real numbers is denoted by $\mathbb{R}$. Let $A = [a_{ij}] \in \mathbb{R}^{n \times n}$, with $n > 0$, its transpose is $A^\intercal$, whereas $a_{ij} \in \mathbb{R}$ denotes its entry in position (i, j). Assume A is symmetric, $A \succ 0$ ($A \succeq 0$) denotes A positive (semi-)definite. Let $\|A\|_2$ and $\|A\|_F = \sqrt{\text{trace}\{A^\intercal A\}}$

be the Euclidean and Frobenius norms, then it holds that $\|A\|_2 \leq \|A\|_F$. Let $B \in \mathbb{R}^{n\times n}$, $A \otimes B = [a_{ij}B] \in \mathbb{R}^{2n\times 2n}$ denote the Kronecker product between A and B, with i and $j = 1, 2, \ldots, n$. The sign operator $\text{sign}(a)$ is understood in the Filippov sense [22], such that $\text{sign}(a) = 1$ if $a > 0$, -1 if $a < 0$, otherwise it is set-valued as follows $\text{sign}(a) \in [-1, 1]$. I_n denotes the n-dimensional identity matrix. 1_n and 0_n are the all 1, and all 0, n-dimensional column vectors. Let $x \in \mathbb{R}^n$, and $A \succ 0$, and $h > 0$, the Jensen inequality for the integral terms Lemma 2.1 in [26] states that

$$-h\int_0^h x(s)^\intercal A x(s)ds \leq -\left(\int_0^h x(s)ds\right)^\intercal A\left(\int_0^h x(s)ds\right). \tag{7}$$

1.5. Nomenclature

For the sake of clarity, the list of variables of the considered nonlinear model of MG, expressed in the *d-q* (direct-quadrature) reference frame, is provided below. The reader is referred to Figure 1 for a graphical explanation of the meaning of some variables. The considered nomenclature for the DG variables is as follows:

ω_{com}: Speed of the common rotating reference frame
ω_i: Speed of the rotating reference frame of the i-th DG
δ_i: Angle between the local and common reference frames
v_{ni}, ω_{ni}: Voltage and frequency secondary control commands;
v_{ki}, i_{ki}: 3-ph voltages and currents at node k of the i-th DG
v_{kdi}, v_{kqi}: *d-q* voltages of the i-th DG at node k
i_{kdi}, i_{kqi}: *d-q* currents of the i-th DG at node k
$k = l, o, b$: Denote the input "$k = l$", output "$k = o$" and bus node "$k = b$"of a DG
ω_0, v_0: Desired voltage and frequency secondary restoration values
P_i, Q_i: Active and reactive powers dc-components at the output node of the i-th DG
v^*_{odi}, v^*_{oqi}: *d-q* voltage set-points of the i-th DG
ψ_{di}, ψ_{qi}: *d-q* voltage error's integral of the i-th DG
i^*_{ldi}, i^*_{lqi}: *d-q* current set-points of the i-th DG
ϕ_{di}, ϕ_{qi}: *d-q* current error's integral of the i-th DG

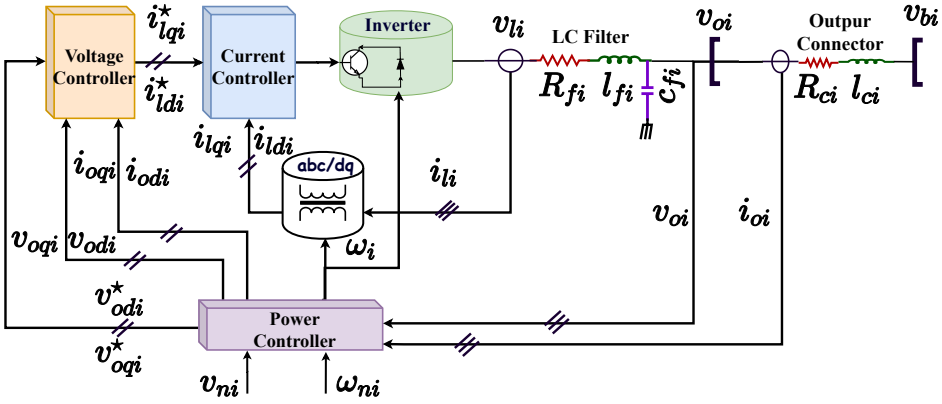

Figure 1. Primary control block diagram of an inverter-based Distributed Generator (DG).

2. Microgrid (MG) Modeling for Secondary Control Design

An MG is a cyber-physical system in which physical and software components are deeply intertwined. At the physical level, an MG is a geographically distributed power system consisting of DGs and loads connected by transmission lines. On the other hand, the supervisory and control algorithms, and in particular the secondary control layer, run over a communication infrastructure as shown in Figure 2.

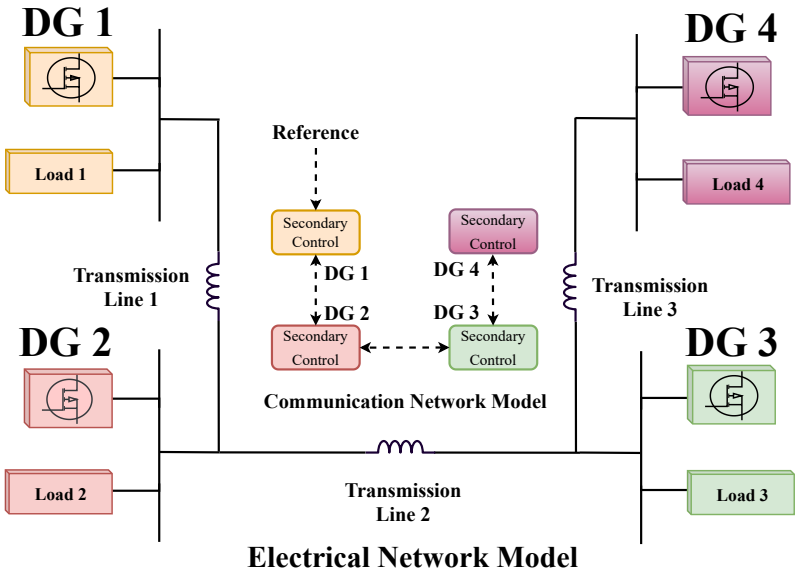

Figure 2. MG cyber-physical representation for secondary control purposes.

An inverter-based DG includes a 3-ph power converter in which the DC side is connected to a dc power source (e.g., photovoltaic panels [27], fuel cell system [28] or a wind turbine [8]), while its AC side is connected to the 3-phase power grid by the series of the coupling and the output filters, see Figure 1.

The Primary Control layer consists of three nested feedback control loops that aim to adjust the power, voltages, and currents injected within the main grid. The behaviour of a primary controlled DG is generally nonlinear. This is because the current and voltage control loops are expressed in the d-q local DG reference frame, rotating at the frequency ω_i [29]. The Secondary Control layer aims at generating the commands/references for the inner Primary Control layer. In particular, through the signals ω_{ni} and v_{ni}, the local DG frequencies ω_i and the direct voltage components v_{odi} should be restored to their respective set-points ω_{ref} and v_{ref}. In general, the phase angle δ_i of each DG i is expressed with respect to a specifically selected DG considered as the common reference frame. Let ω_{com} be the rotating speed of the common reference frame, then one has that

$$\frac{d\delta_i(t)}{dt} = \omega_i(t) - \omega_{\text{com}}. \tag{8}$$

The local frequency and voltage droop primary control characteristics are as follows

$$\omega_i(t) = \omega_{ni}(t) - m_i \cdot P_i(t) \tag{9}$$
$$v^*_{odi}(t) = v_{ni}(t) - n_i \cdot Q_i(t) \tag{10}$$
$$v^*_{oqi}(t) = 0, \tag{11}$$

where m_i and n_i represent the droop power coefficients, which aim to mimic the generator's inertia. Then, $P_i(t)$ and $Q_i(t)$ denote the DC components of active and reactive power flows at the DG outputs. A low-pass process with cut-off frequency $\omega_{ci} \ll \omega_i \leqslant \omega_{ni}$ is designed to obtain $P_i(t)$ and $Q_i(t)$ as next

$$\frac{dP_i(t)}{dt} = -\omega_{ci}P_i(t) + \omega_{ci}\left(v_{odi}(t) \cdot i_{odi}(t) + v_{oqi}(t) \cdot i_{oqi}(t)\right) \tag{12}$$
$$\frac{dQ_i(t)}{dt} = -\omega_{ci}Q_i(t) + \omega_{ci}\left(v_{oqi}(t) \cdot i_{odi}(t) - v_{odi}(t) \cdot i_{oqi}(t)\right). \tag{13}$$

Finally, the inner voltage and current primary control loops consists of cascaded PI controllers combined with feed-forward compensation terms. The voltage control is as follows

$$\frac{d\psi_{di}(t)}{dt} = k_{ivi}(v^*_{odi}(t) - v_{odi}(t)) \tag{14}$$

$$\frac{d\psi_{qi}(t)}{dt} = k_{ivi}(v^*_{oqi}(t) - v_{oqi}(t)) \tag{15}$$

$$i^*_{ldi}(t) = \psi_{di}(t) + k_{pvi}(v^*_{odi}(t) - v_{odi}(t)) + k_{fvi}i_{odi}(t) - \bar{\omega}C_{fi}v_{oqi}(t) \tag{16}$$

$$i^*_{lqi}(t) = \psi_{qi}(t) + k_{pvi}(v^*_{oqi}(t) - v_{oqi}(t)) + k_{fvi}i_{oqi}(t) + \bar{\omega}C_{fi}v_{odi}(t), \tag{17}$$

whereas the inner current controller satisfies the next relations

$$\frac{d\phi_{di}(t)}{dt} = k_{ici}(i^*_{ldi}(t) - i_{ldi}(t)) \tag{18}$$

$$\frac{d\phi_{qi}(t)}{dt} = k_{ici}(i^*_{lqi}(t) - i_{lqi}(t)) \tag{19}$$

$$v^*_{ldi}(t) = \phi_{di}(t) + k_{pci}(i^*_{ldi}(t) - i_{ldi}(t)) - \bar{\omega}L_{fi}i_{lqi}(t) \tag{20}$$

$$v^*_{lqi}(t) = \phi_{qi}(t) + k_{pci}(i^*_{lqi}(t) - i_{lqi}(t)) + \bar{\omega}L_{fi}i_{ldi}(t), \tag{21}$$

where $\bar{\omega}$ is specified as the nominal angular frequency of the MG. Lastly, L_{fi} and C_{fi} denote the inductance and capacitance of the coupling filter drawn in Figure 1, and k_{pvi}, k_{ivi}, k_{fvi} and k_{pci}, k_{ici}, k_{fci} denotes, respectively, the proportional, integral and feed-forward gains of those controllers.

Finally, the voltage and current dynamics associated with the local LC filter and the output connector are

$$\frac{di_{ldi}(t)}{dt} = -\frac{R_{fi}}{L_{fi}}i_{ldi}(t) + \frac{1}{L_{fi}}(v_{ldi}(t) - v_{odi}(t)) + \omega_i(t)i_{lqi}(t) \tag{22}$$

$$\frac{di_{lqi}(t)}{dt} = -\frac{R_{fi}}{L_{fi}}i_{lqi}(t) + \frac{1}{L_{fi}}\Big(v_{lqi}(t) - v_{oqi}(t)\Big) - \omega_i(t)i_{ldi}(t) \tag{23}$$

$$\frac{dv_{odi}(t)}{dt} = \frac{1}{C_{fi}}(i_{ldi}(t) - i_{odi}(t)) + \omega_i(t)v_{lqi}(t) \tag{24}$$

$$\frac{dv_{oqi}(t)}{dt} = \frac{1}{C_{fi}}\Big(i_{lqi}(t) - i_{oqi}(t)\Big) - \omega_i(t)v_{ldi}(t) \tag{25}$$

$$\frac{di_{odi}(t)}{dt} = -\frac{R_{ci}}{L_{ci}}i_{odi}(t) + \frac{1}{L_{ci}}(v_{odi}(t) - v_{bdi}(t)) + \omega_i(t)i_{oqi}(t) \tag{26}$$

$$\frac{di_{oqi}(t)}{dt} = -\frac{R_{ci}}{L_{ci}}i_{oqi}(t) + \frac{1}{L_{ci}}\Big(v_{oqi}(t) - v_{bqi}(t)\Big) - \omega_i(t)i_{odi}(t), \tag{27}$$

where, in accordance with Figure 1, $v_{bdi}(t)$, $v_{bqi}(t)$ denote the d-q voltages at the connection bus. Let $v^*_{ldi}(t)$ and $v^*_{lqi}(t)$ in (20) and (21) express the smooth signals presented by inner current primary control loop, whereas $v_{ldi}(t)$ and $v_{lqi}(t)$ in (22) and (25) represent the effective non-smooth dispatched voltages of the inverter at the AC port after a high frequency PWM process. It is worth mentioning that, since the switching frequencies of power bridges are very high, the inverter dynamics can safely be ignored by comparing the MG dynamics. Hence, according to the averaging principle, (20) and (21) can be replaced for v_{ldi} and v_{lqi} into (22) and (23), more details can be found in [30,31].

Henceforth, the following reasonable assumption is assumed to hold.

Assumption 1. *Consider the primary controlled MG (8)–(21). Let a priori known bounds Π^P and Π^Q exist, such that, for each DG the active and reactive powers at the DG's output node "o" are assumed to be bounded by*

$$\left|v_{odi}i_{odi} + v_{oqi}i_{oqi}\right| \leqslant \Pi^P \quad , \quad \left|v_{oqi}i_{odi} - v_{odi}i_{oqi}\right| \leqslant \Pi^Q. \tag{28}$$

Remark 1. *Assumption 1 is justified because the power flowing in the lines and/or absorbed by the load is bounded everywhere due to: (a) the passive behaviour of loads and lines; (b) the bounded operating range of the inverter voltages and currents due to their physical limits; (c) the presence of protection apparatus and the inner voltage and current primary control loops. This keeps the power flows within pre-specified ranges as discussed for instance in [11,30,32].*

As discussed in [8,11,15,31], the cascaded voltage and current control loops in, resp., (14)–(17) and (18)–(21), are theoretically justified based on time-scale separation techniques. In particular because of the filter inductance L_{fi} in (22), and because the inverse of the current integral gain $1/k_{ici}$ in (18) can reasonably be considered small enough, then from (18), (20), (22) the following the Singular Perturbation analysis takes place

$$\epsilon\left(\tfrac{d}{dt}\begin{bmatrix} i_{ldi}(t) \\ \phi_{di}(t)\end{bmatrix} - \begin{bmatrix}(\omega_i(t)-\bar{\omega})i_{lqi} \\ 0\end{bmatrix}\right) = \begin{bmatrix}-R_{fi}-k_{pci} & 1 \\ -1 & 0\end{bmatrix}\begin{bmatrix} i_{ldi}(t) \\ \phi_{di}(t)\end{bmatrix} + \begin{bmatrix}1 \\ 1\end{bmatrix} i^*_{ldi}(t),$$

where $\epsilon = \max\{L_{fi}, 1/k_{ici}\}$ is the so-called perturbation parameter. Now according to the singular perturbation method and setting $\epsilon = 0$, the quasi steady-state behaviour of the current fast dynamics can be obtained as

$$\begin{bmatrix} i_{ldi}(t) \\ \phi_{di}(t)\end{bmatrix} \equiv \begin{bmatrix} 1 \\ -k_{pci}-R_{fi} \quad -1\end{bmatrix} \cdot i^*_{ldi}(t). \tag{29}$$

Hence, at the quasi-steady mode the current control induces the inverter to send its set-point (16) almost immediately despite the inherent connection between the d and q component. Likewise one also obtains that $i_{lqi}(t) \equiv i^*_{lqi}(t)$. From (16), (24) and (29) the reduced-order relation between v_{odi} and the control input v_{ni} is

$$\dot{v}_{odi}(t) = \frac{1}{C_{fi}}\Big((\omega_i(t)-\bar{\omega})v_{oqi}(t) + \psi_{di}(t) + (k_{fvi}-1)i_{odi}(t)\Big) + \frac{k_{pvi}}{C_{fi}}(v_{ni}(t) - v_{odi}(t)). \tag{30}$$

For later use, we express (30) in the next augmented form

$$\begin{bmatrix}\dot{v}_{odi}(t) \\ \ddot{v}_{odi}(t)\end{bmatrix} = A\begin{bmatrix} v_{odi}(t) \\ \dot{v}_{odi}(t)\end{bmatrix} + B\left(\frac{k_{pvi}}{C_{fi}}(\dot{v}_{n_i}(t) - \dot{v}_{odi}) + \dot{w}_i(t)\right), \tag{31}$$

with

$$A = \begin{bmatrix}0 & 1 \\ 0 & 0\end{bmatrix}, \quad B = \begin{bmatrix}0 \\ 1\end{bmatrix}, \tag{32}$$

where $\dot{v}_{n_i}$ is the actual voltage secondary control command and

$$\dot{w}_i(t) = \dot{\omega}_i(t)v_{oqi}(t) + (\omega_i(t)-\bar{\omega})\dot{v}_{oqi}(t) + (k_{fvi}-1)\dot{i}_{odi}(t) \qquad |\dot{w}_i(t)| \leqslant W_i \tag{33}$$

plays as a matched unknown term accounting perturbation, parameter uncertainties, unmodelled dynamics, as well as chances in the MG working-point. Let us further note that due to Assumption 1, and the inherent boundedness of the MG variables enforced by the Primary Control, which makes the DG's frequency and voltages smooth, with bounded derivatives, then the existence of a sufficiently large constant W_i such that (33) holds if fairly reasonable.

MG's Network Models

To achieve the Secondary Control objectives in a distributed way, DGs are assumed to be provided with computing and communication facilities embedded within their local controllers. Thus, each DG plays the role of autonomous *agent* over a networked cyber-physical system. Agents communicate over a network in which topology is encoded by a real-weighted graph $\mathcal{G}_N = (\mathcal{V}, \mathcal{E}_N)$, where $\mathcal{V} = 1, 2, \ldots, N$ is the set of local secondary controllers (or without loss of generality simply DGs), whereas $\mathcal{E}_N$ is the set of the available communication links between DGs, and $\mathcal{A} = [\alpha_{ij}] \in \mathbb{R}^{N \times N}$ is the so-called adjacency matrix, where $\alpha_{ij} = 1$ if $(i, j) \in \mathcal{E}_N$, namely if DG i can receive data delivered by DG j, otherwise $\alpha_{ij} = 0$. Accordingly with the leader–follower paradigm, we further assume the existence of a root node, labelled by 0 in the augmented graph $\mathcal{G}_{N+1}(0 \cup \mathcal{V}, \mathcal{E}_{N+1})$, which aims to provide the secondary control set-points to a non-empty set of DGs. Accordingly with Appendix A, where preliminary results on Graph Theory are provided, in the remainder, $\mathcal{L}$ and $\mathcal{L}_{N+1}$ denote the Laplacian matrices associated with $\mathcal{G}_N$ and $\mathcal{G}_{N+1}$. In the remainder, communications will be assumed to be affected by the network-induced time-varying delays. Further details on that will be given in the next section.

3. Voltage Secondary Control Design

Let the desired voltage set-point provided by the virtual node 0 be denoted by $v_0 \equiv v_{\text{ref}} > 0$. In the absence of a secondary control loop, and by assuming the voltage set-point globally available to each DG, thus by letting $v_{ni} \equiv v_0$, it can be noted that, due to the droop-power terms in (10) and (11) and the voltage drops in (30), at the resulting equilibrium $v_{di}(t)$ will be smaller than v_0, thus restoration is needed. Our control objective can thus be summarized as follows

$$\lim_{t \to \infty} v_{odi}(t) = v_0 \qquad \forall\, i = 1, 2, \ldots, N, \tag{34}$$

where v_0 is available only to a subset of DGs. To globally solve the secondary control problem (34) in a distributed way and by accounting network-induced delays in the communication links the next control protocol is proposed

$$\dot{v}_{n_i}(t) = \frac{C_{fi}}{k_{pvi}}(k \cdot u_i(t) - m_i \cdot \text{sign}(s_i(t))), \tag{35}$$

where $s_i(t)$ is the desired integral sliding mode control manifold designed as follows

$$s_i(t) = \dot{v}_{odi}(t) + v_{odi}(t) - z_i(t) \tag{36}$$

$$\dot{z}_i(t) = k \cdot u_i(t) + \frac{k_{pvi}}{C_{fi}} \cdot \dot{v}_{odi}(t), \quad z_i(0) = -\dot{v}_{odi}(0) - \dot{v}_{odi}(0), \tag{37}$$

and

$$\begin{aligned} u_i(t) = \; & -\textstyle\sum_{j=0}^{N} \alpha_{ij} \Big[v_{odi}(t - \tau_{ij}(t)) - v_{odj}(t - \tau_{ij}(t)) \Big] + \\ & -2 \textstyle\sum_{j=0}^{N} \alpha_{ij} \Big[\dot{v}_{odi}(t - \tau_{ij}(t)) - \dot{v}_{odj}(t - \tau_{ij}(t)) \Big], \end{aligned} \tag{38}$$

where $m_i > 0$ and $k > 0$ are some constant gains to be designed, and α_{ij} denotes whether DG j is enabled to communicate with DG i, namely $\alpha_{ij} = 1$ if $(i, j) \in \mathcal{E}_{N+1}$. Finally $\tau_{ij}(t)$ is the time-varying delay associated with the communication from DG j to DG i, with $(i, j) \in \mathcal{E}_{N+1}$.

Remark 2. *It is worth remarking that the DG's output voltage derivatives are not available for measurements. However, they can easily be estimated and then used for output feedback purposes by means of differentiators implemented within each local controller. Following [33], and thanks to the finite-time convergence properties provided by the well-known Levant's exact differentiator,*

$$\begin{array}{rcl} \dot{\hat{v}}_{odi}(t) & = & -c_{i,1} \cdot \sqrt{|v_{odi}(t) - \hat{v}_{odi}(t)|} \cdot \text{sign}(v_{odi}(t) - \hat{v}_{odi}(t)) + \omega_i(t) \\ \dot{\omega}_i(t) & = & -c_{i,2} \cdot \text{sign}(v_{odi}(t) - \hat{v}_{odi}(t)) \end{array} \tag{39}$$

$$c_{i,1} > 1.5\sqrt{C_i}\ ,\ c_{i,2} > 1.1C_i, \tag{40}$$

where if C_i large enough, it results that, after a finite interval of time the estimation $\dot{\hat{v}}_{odi}(t)$ coincides with the true value $\dot{v}_{odi}(t)$. This is the reason why in (35)–(38) the quantities $\dot{v}_{odi}(t)$ are treated as if they were known.

Remark 3. *According to Figure 2, the DGs dynamics are coupled with each other due to the interconnecting power lines and are also affected by the local utilities. Although (9)–(27) do not explicitly show this coupling, these effects can be encoded by the bus voltages v_{bi} [31]. Let us further note that, differently to [9,10], where these voltages were considered to be known and then compensated using feedback-linearization/feedforward approaches, in the present work they are supposed to be unknown. It is also worth mentioning that the considered model is strongly nonlinear because the primary control is designed in the d-q reference frame. Thus, due to its inherent nonlinear behaviour and because of, to the best of our knowledge, all the available time-delay tolerant secondary controllers are linear, then they can provide stable results only in the local sense. On the contrary, here, by means of the proposed robust control protocol, we can account for both the presence of communication delays and model nonlinearities/uncertainties without any model approximation, thus providing stability in the large sense.*

Remark 4. *The design (35)–(38) is inspired by the robustification method proposed in [22] for arbitrary distributed consensus and optimization problems. Differently to that, here also the presence of communication delays is accounted for. The discontinuous term consists of an ISMC control term that aims to enforce each DG to behaves as a nominal multi-agent system, namely such that $\ddot{v}_i = k \cdot u_i$. Then, $u_i(t)$ is properly designed to fulfil (34) under the given communication topology and delays.*

For later use, the collection of delays affecting the available communication links between the leader (node 0) and the generic DG j will be denoted by the set $\mathcal{T}(t) = \{\tau_1, \tau_2, \ldots, \tau_q\}$, where each element $\tau_l(t) \in \mathcal{T}(t)$ is such that

$$\tau_l(t) = \tau_{i0}(t),\ \ \forall\, i : (i,0) \in \mathcal{E}_{N+1},\ l = 1,2,\ldots,q. \tag{41}$$

Then, we indicate with $\mathcal{S}(t) = \{\sigma_1, \sigma_2, \ldots, \sigma_m\}$ the collection of delays affecting the oriented communications among DGs, and where $\sigma_g(t) \in \mathcal{S}(t)$ is such that

$$\sigma_g(t) = \tau_{ij}(t),\ \forall\ (i,j) \in \mathcal{G}_N,\ \forall\ g = 1,2,\ldots,m \tag{42}$$

Note that the indexes $m \leq N(N-1)$ and $q \leq N$ equal their maximum values only if $\mathcal{G}_{N+1}$ is a complete graph, and all the delays, for a given time t, are different. The common assumption of slowly-varying, bounded delays is made in [15,23,24,34,35].

Assumption 2. *Let a priori known bounds $\tau_l^\star$, $\sigma_g^\star$, δ_l, $\delta_g > 0$ exist, such that, for each delay $\tau_l \in \mathcal{T}$ and $\sigma_g \in \mathcal{S}$,*

$$\begin{array}{l} \tau_l \equiv \tau_{i0} \in \left[0, \tau_l^\star\right),\ |\dot{\tau}_{i0}| \leq \delta_l < 1 \\ \sigma_g \equiv \tau_{ij} \in \left[0, \sigma_g^\star\right),\ |\dot{\tau}_{ij}| \leq \delta_g < 1 \end{array}\ ,\ \forall\ t \geq 0. \tag{43}$$

To correlate the data received from a DG for feedback purposes we further assume that:

Assumption 3. *Each communication delay $\tau_{ij}(t)$ is detectable for all $t \geq 0$, and $(i,j) \in \mathcal{G}_{N+1}$.*

Remark 5. *Communication protocols used to include the data-packet timestamp, thus the requirement of detectable delays is costless [36]. Once the delay is detected by means of local buffers each controller is enabled to retrieve its own state at that time and performs (38). These averaging laws are common in networked applications with multiple delays [15,23,24,37], and others.*

The main results of the present paper are now presented:

Theorem 1. *Consider an MG of N DGs in which voltage dynamics satisfy (31), under the voltage control (35)–(38). Let the communication topology $\mathcal{G}_N$ be connected and undirected. Let node 0 be a root node over the augmented graph $\mathcal{G}_{N+1}(0 \cup \mathcal{V}, \mathcal{E}_{N+1})$. Let the communications subjected to heterogeneous time-varying delays $\tau_{ij}(t)$ with given upper-bounds $\tau_l^\star$, $\sigma_g^\star$, and $\delta_l < 1$ and $\delta_g < 1$ as in (43). Let Assumptions 1, 2, 3, be in force. Let $m_i > W_i$ in (33). If the matrix inequality problem (1)–(6) admits a feasible solution with respect to $k > 0$, $\eta > 0$, and the symmetric positive definite matrices P, Q_l, Q_g, R_g, W_l, $W_g \in \mathbb{R}^{2N \times 2N}$, then the voltage restoration objective (34) can be globally uniformly asymptotically achieved.*

Proof of Theorem 1. See the Appendix D. □

Remark 6. *The matrix inequality problem (1)–(6) is strongly non-linear with respect to k, thus standard convex optimization solvers will fail in finding their solutions because of the quadratic dependence from k of (5), and (6). However, for a given k, (1)–(6) degenerates into a set of LMIs, thus is solvable by means of standard convex optimization solvers, as for instance the well-known* `feasp` *MATLAB's LMI solver which is based on the Nesterov and Nemirovski's Polynomial Projective Method. The following Algorithm 1 is thus proposed to provide a method to find systematically, if it exists, the maximal feasible gain $k^\star$ for (35)–(38) such that, for the given delays' bounds, the fulfilment of the control objective is guaranteed.*

Before presenting Algorithm 1 the next instrumental lemma is provided.

Lemma 1. *Consider an undirected connected communication graph $\mathcal{G}_N(\mathcal{V}, \mathcal{E}_N)$ and its augmented graph $\mathcal{G}_{N+1}(0 \cup \mathcal{V}, \mathcal{E}_{N+1})$ and $\mathcal{V} = 1, 2, \ldots, N$. Let node 0 be a root node over $\mathcal{G}_{N+1}$. Consider the matrices $A_l(k)$, and $\hat{A}_g(k)$ as in (1) and the matrix $\Phi(k)$ as in (2). Then $\Phi(k)$ is Hurwitz $\forall$ $k > 0$.*

Proof. See Appendix C. □

Corollary 1. *Assume the condition of Theorem 1 to be satisfied. Hence a $k = k^\star$ exists such that, for the given delays' bounds the control objectives can be fulfilled. Then, Algorithm 1 will find such a feasible gain value $k^\star$; (b) Let $\hat{H} = \sum_{g=1}^{m} W_g + \sum_{l=1}^{q} W_l$ and $k = k^\star$, an estimation of the maximum delay tolerated by the control system is given by*

$$\tau^\star = \min_{\forall\, l,g} \left\{ \frac{\left\| (P\Phi(k)^\intercal + P\Phi(k)) + \sum_{l=1}^{q} Q_l + \sum_{g=1}^{m} Q_g \right\|_2}{\left\| \sum_{g=1}^{m} R_g \right\|_F}, \frac{\|(1-d_l)Q_l\|_2/\eta}{\left\| A_l(k)^\intercal \hat{H} A_l(k) \right\|_F}, \frac{\left\|(1-d_g)Q_g\right\|_2/\eta}{\left\| A_g(k)^\intercal \hat{H} A_g(k) \right\|_F} \right\}. \quad (44)$$

Proof. Consider the LMI (5). Independently from the given $k > 0$ and $\eta > 0$, the delays' bounds, and the positive definite matrices W_l and W_g, there will always exist a sufficiently large positive definite matrix $Q_l \succ 0$ such that $-(1-\delta_l)Q_l + \eta(A_l(k)^\intercal \sum_{g=1}^{m} \sigma_g^\star W_g + \sum_{l=1}^{q} \tau_l^\star W_l A_l(k)) \prec 0$, $\forall$ l. It follows that (5) is always feasible. The same can be concluded for (6) and $\forall$ g. Consider now the LMIs (3) and (4), which are coupled to each other by means of the matrices $R_g \succ 0$, and which play as dummy variables. Thus by substituting the right-hand side of (4) into (3), and by letting $\hat{Q} = (\sum_{l=1}^{q} Q_l + \sum_{g=1}^{m} Q_g + \eta \cdot A_0^\intercal \left(\sum_{g=1}^{m} \sigma_g^\star W_g + \sum_{l=1}^{q} \tau_l^\star W_l \right) A_0)$, the following LMI takes place: $\Phi^\intercal P + P\Phi + \hat{Q} \prec 0$. Thus, because of Lemma 1, provided in Appendix B, Φ is Hurwitz, and $\hat{Q}$ is, by construction, positive definite, then a matrix $P \succ 0$ can be found, satisfying the resulting Lyapunov

equation $\Phi^\intercal P + P\Phi + \hat{Q} = -\epsilon I_{2N}$, $\forall\, \epsilon > 0$. Thus, (3) is also always feasible. It follows that, if a feasible gain $k^\star$ exists, by means of Algorithm 1, the feasibility problem associated with (1)–(6) can be numerically studied iteratively for different k, until such a value $k = k^\star$ is found. If the actual k does not correspond with a feasible solution then k is decreased by $\Delta k > 0$, and the routine is repeated. On the other hand, if k becomes smaller than or equal to zero, it means that for the given delays' bounds, Δk and $\bar{k}$, a feasible $k^\star$ does not exist. This confirms sentence (a).

Once a feasible solution for (1)–(6) is found, a lower estimation of the maximum delay tolerated $\tau^\star$ by the system can be easily derived as follows: (1) Let us first replace such a solution on (1)–(6); (2) Then, by substituting $\tau^\star(\sum_{g=1}^{m} W_g + \sum_{l=1}^{q} W_l)$ to $\sum_{g=1}^{m} \sigma_g^\star W_g + \sum_{l=1}^{q} \tau_l^\star W_l$, a set of inequality in which the only unknown variable is $\tau^\star$ takes place; (3) Finally, by solving for $\tau^\star$, by applying norms to the numerator and denominator and because $\|\cdot\|_2 \leq \|\cdot\|_F$, after manipulations, (44) is obtained. □

Remark 7. *The achievement of the voltage restoration condition* (34) *through the proposed robust control protocol* (35)–(38) *does not affect the stability of the DGs' frequencies. In fact, because of the presence of the droop power control* (9)–(10)*, which guarantees the MG synchronism and stability to load changes/variations, and because the achievement of* (34) *simply implies some smooth changes on* $P_i(t)$ *in accordance with* (12)*, now* $v_{odi} \to v_0$*. Then, the achievement of the voltage restoration will simply modify the actual frequency equilibria, which will correspond, following the analysis in [2], to the next quantity* $\omega_i(\infty) = \omega_{ni} - \sum_i P_i(t)/(\sum_i m_i^{-1})$*. Let us further note that, because at each time t the total power in the MG is time-invariant, then the current's steady equilibria will change accordingly, as well. The results shown in Figure 3 corroborate these statements.*

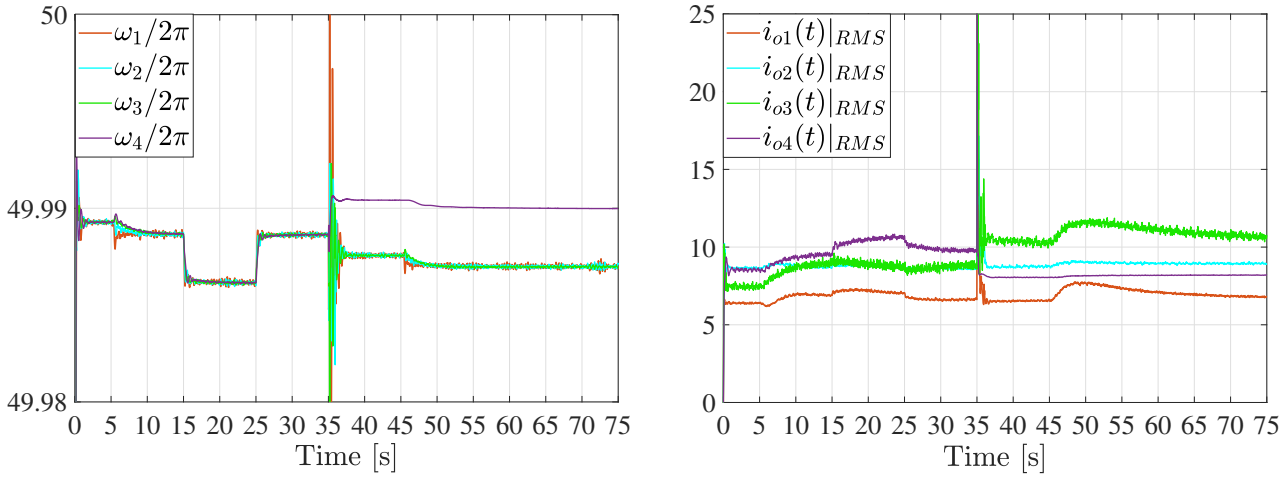

Figure 3. (**a**) Frequencies of the DG's output voltages measured by 3-phase Phase Locked Loop sensors; (**b**) RMS inverters' output currents.

4. Results and Discussion

4.1. Test Rig Design

The proposed voltage control is tested on a realistic MG model developed by means of the *Simscape Power Systems*^{TM} MATLAB/Simulink toolbox. Figure 2 depicts the schematics of the considered inverter-based MG. Each DG model comprises a *3-ph An IGBT bridge* with 10 kVA of rated power provided by a 800 V dc-source. *PWM Generators* with 2 kHz carrier are employed to control the switching devices. In accordance with Equations (9)–(21) and (35)–(38), the primary and secondary controls are described in the local rotating reference frames by means of *d-q* Parks' Transformations. The dynamics of the LC filters (22)–(25), and of the output connectors (26) and (27), and the 3-ph power lines are instead formulated in the *abc* frame by using *3-ph Series RLC Branches*. Loads consists of *3-ph Parallel RLC*

Loads. The current and voltage outputs of the inner voltage and current PIs, as well as the PWM modules, are saturated in accordance with the DGs' rated powers, resp., $380V_{ph-ph}$, 32A. The MG and DGs parameters are listed in Table 1. Lastly, to show the robustness of the proposed control rule to sudden unplanned events, a *3-ph to ground fault* on Line 3 of Figure 2 will be scheduled throughout the simulation. Then, due to the surge of transient currents generated by the faults and according to the delays of protection devices, 10 ms later, two *circuit breakers* located at the branch buses of DG 3 and DG 4 will isolate the MG in two portions accordingly with the fault location.

The Runge-Kutta fixed-step solver is employed in the MATLAB environments to carry out the simulation with sampling time $T_s = 2\,\mu s$. The primary and secondary controllers have been discretized using a sampling step $\bar{T}_s = 500\,\mu s$. It is also worth mentioning that all the measurements used for feedback control are affected by realistic measurement noise. In particular, the MG currents and voltages measurements were first converted into the $4 \div 20\,mA$ wired protocol with power transmission equal to 0.2 W, and were then corrupted by an Additive White Gaussian Noise with a realistic Signal-to-Noise Ratio of 90 dB [11].

The communication topology is chosen to be connected and undirected as in Figure 2. Only DG 1 can access the voltage set-point v_0 from the virtual node 0. Communication delays are time-varying such that, for each oriented link $(i,j) \in \mathcal{E}_{N+1}$, $\dot{\tau}_{ij}(t)$ is randomly uniformly distributed within the open-interval $(-1,1)$. The delays' bounds in (43) are $\tau_l^\star = \sigma_g^\star = 0.03\,s$, and $d_l = d_g = 0.999$, $\forall\, l$ and g.

Table 1. Parameters Values for the Microgrid Test System [11].

DG's Parameters		**DG 1**	**DG 2**	**DG 3**	**DG 4**
Droop Control	m_p	10×10^{-5}	6×10^{-5}	4×10^{-5}	3×10^{-5}
	n_Q	1×10^{-2}	1×10^{-2}	1×10^{-2}	1×10^{-2}
Voltage Control	k_{pv}	0.4	0.4	0.4	0.4
	k_{iv}	500	500	500	500
	k_{fv}	0.5	0.5	0.5	0.5
Current Control	k_{pc}	0.4	0.4	0.4	0.4
	k_{ic}	700	700	700	700
LC Filter [Ω], [mH], [μF]	R_f	0.1	0.1	0.1	0.1
	L_f	1.35	1.35	1.35	1.35
	C_f	50	50	50	50
Connector [Ω], [mH]	R_c	0.03	0.03	0.03	0.03
	L_c	0.35	0.35	0.35	0.35
Lines [Ω], [μH]		Line 1		Line 2	Line 3
	R_{l1}	0.23	R_{l2}	0.23	R_{l3} 0.23
	L_{l1}	318	L_{l2}	324	L_{l3} 324
Loads [kW], [kVar]		Load 1		Load 2	Load 3	Load 4
	P_{L1}	3	P_{L2}	3	P_{L3} 2	P_{L4} 3
	Q_{L1}	1.5	Q_{L2}	1.5	Q_{L3} 1.3	Q_{L4} 1.5

4.2. Voltage Secondary Control Implementation

Algorithm 1 has been implemented in the MATLAB environment, and the LMI problem (1)–(6) built by means of the `lmiedit` symbolic interface. The implementation of step (b) takes instead the advantage of the `feasp` LMI solver. Algorithm 1 is initialized with $\bar{k} = 5$ and $\Delta k = 0.01$. For the given delays' bounds and the communication topology

$\mathcal{G}_{N+1}$, it results in an optimal maximal gain $k = k^\star = 3.42$, which corresponds to a delay stability margin of $\tau^\star = 0.0781$s. On the other hand, the discontinuous gain m_i has been set equal to 140. It is also worth mentioning that to reduce the so-called chattering effect the sign operator in (35) is approximated as a sigmoidal function, namely $\text{sign}(a) \approx a/(|a| + \varepsilon)$ with $\varepsilon = 0.01$, and where $a \in \mathbb{R}$ denotes the operator argument. Finally the differentiators gains in (40) are chosen to be large enough. In particular, we set $C_i = 1000$.

4.3. Case Study

The system is tested for 75s, and the delays are randomly initialized as next $\tau_{ij}(0) \in [0.5\tau^\star, \tau^\star]$. The list of events scheduled throughout the test is displayed:

- Step 1 ($t = 0$ s): Only the primary control is active with $\omega_{ni} = 2\pi 50$ Hz, $v_{ni} = 220\,\text{V}_{\text{RMS}}$ (per phase rms);
- Step 2 ($t = 5$ s): The voltage control with v_{ni} as in (35)–(38) and $v_0 = 220\,\text{V}_{\text{RMS}}$ is activated;
- Step 3 ($t = 15/25$ s): An additional load (P_{L3}, Q_{L3}) is connected/disconnected at the bus 3;
- Step 4 ($t = 35$ s): A 3-ph to ground fault occurs on the Line 3;
- Step 5 ($t = 35.1$ s): Over-current protection devices isolate Line 3, thus DG4 results electrically isolated;
- Step 6 ($t = 45$ s): The set-point for the voltage Secondary Control is changed to $v_0 = 225\,\text{V}_{\text{RMS}}$;

Consider Figure 4a. In the first five seconds, when only the primary control is active, all the DG voltages are less than the reference value of $220\,\text{V}_{\text{RMS}}$. It is evident that restoration is needed. Once at $t = 5$ s the proposed voltage control is activated, promptly the DGs' output voltages are globally, asymptotically, restored to the desired setpoint, despite the communication delays. Then, the MG operating working points change after the connection/disconnection of the additional load (P_{L3}, Q_{L3}) by means of a 3-ph breaker. This verifies that the proposed controller is robust against unexpected changes of demands. Moreover, at $t = 35$ s also a 3-ph to ground fault is triggered on the line between DG 3 and DG 4. Then, 10 ms later that line is isolated and the MG is sectioned into two sub-MGs, one consisting of DG 1, DG 2, and DG 3 and the respective loads, and another composed only of DG 4 and the local load (P_{L4}, Q_{L4}). From Figure 4a it can be observed that although the occurrence of such a critical event at $t = 35$ s, and the fact that now DG 4 is isolated, all the DG's voltages remain at the desired nominal setpoint $v_{\text{ref}} = 220\,\text{V}_{\text{RMS}}$. Then, at $t = 45$ s such a setpoint is changed to $v_0 = 225\,\text{V}_{\text{RMS}}$. Consequently, all the DG's voltages converge to it. Finally, the time evolution of the voltage secondary control signals is shown in Figure 4b. The results justify that the proposed scheme provides a satisfactory performance and smooth control signals. Following what was stated in Remark 7, and with the aim of showing that the achievement of the voltage restoration by means of the proposed controller does not affect the MG stability, in Figure 3a the DGs' frequencies measured by means of 3-phase Phase-Locked Loop sensors deployed at the DGs' output nodes are drawn. Then, for the sake of completeness, the temporal response of the DGs' RMS currents is also further provided in Figure 3b.

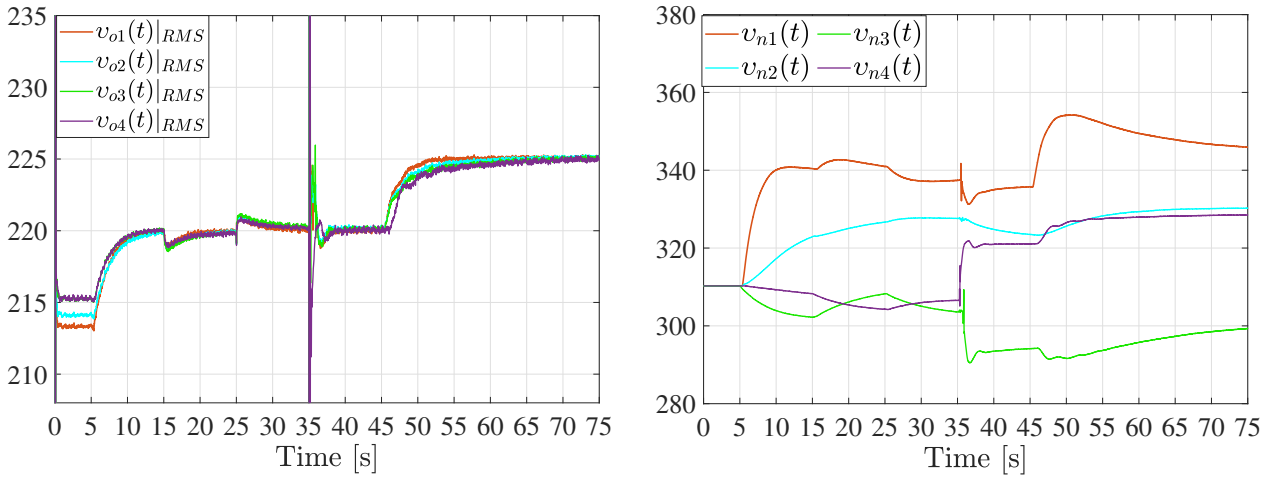

Figure 4. (**a**) RMS inverter's output voltages; (**b**) Secondary voltage restoration control actions.

5. Conclusions

Most of the existing time-delay tolerant MG control protocols are linear. Thus, because an MG is a strongly nonlinear system, all those approaches can only provide stability features in the local sense under additional model approximation or linearization procedures. Our approach instead improves the current State-of-the-Art by providing stability features in the large sense by means of a co-design control method, which inherits both the robustness features of the sliding mode control paradigm and the resilience of the LMI-based controller against network induced time-varying communication delays. Future research activities will be devoted to removing the assumption of slowly varying delay and will consider more general communication topologies. Moreover, extensions of the proposed method to the frequency restoration problem are currently under investigation.

Author Contributions: Conceptualization, M.G. and A.P. (Alessandro Pilloni); methodology, A.P. (Alessandro Pilloni); software, M.G.; validation, M.G. and A.P. (Alessandro Pilloni); formal analysis, A.P. (Alessandro Pilloni); writing—original draft preparation, A.P. (Alessandro Pilloni); writing—review and editing, A.P. (Alessandro Pilloni); visualization, M.G.; supervision, A.P. (Alessandro Pilloni); project administration, A.P. (Alessandro Pilloni); funding acquisition, A.P. (Alessandro Pisano), and E.U. All authors have read and agreed to the published version of the manuscript.

Funding: The research leading to these results has received funding by: Fondazione di Sardegna under project "SISCO" (CUP:F74I19001060007); by the Sardinian Regional Government, by project "Virtual Energy" under call "Cluster top-down actions (POR FESR)", and project MOSIMA (RASSR05871), FSC 2014-2020, annuity 2017, Subject area 3, Action Line 3.1, and POR SARDEGNA FSE 2014-2020-Asse III, Azione 10.5.12, "Avviso di chiamata per il finanziamento di Progetti di ricerca Anno 2017".

Institutional Review Board Statement: Not applicable.

Informed Consent Statement: Not applicable.

Data Availability Statement: Not applicable.

Conflicts of Interest: The authors declare no conflict of interest.

Appendix A. Graph Theory

A directed graph $\mathcal{G}_N(\mathcal{V}, \mathcal{E}_N)$ is a topological tool used to describe pairwise interactions between objects, abstractly referred as *nodes*, or *agents* in the multi-agent research area. The *node set* is $\mathcal{V} = \{1, 2, \ldots, N\}$, whereas the *edges set* $\mathcal{E}_N \subseteq \{\mathcal{V} \times \mathcal{V}\}$ describe the node's pairwise interactions. Let $(i, j) \in \mathcal{E}_N$, we refer to i; and j as the tail and head of the edge. The *adjacency matrix* of $\mathcal{G}_N$ is $\mathcal{A} = [\alpha_{ij}] \in \mathbb{R}^{N \times N}$, and α_{ij} denotes the *edge weight*. If $(i, j) \notin \mathcal{E}$

then $\alpha_{ij} = 0$, otherwise $\alpha_{ij} = 1$. A *directed path* is an alternating sequence of nodes and edges with both endpoints of an edge appearing adjacent to it in the sequence. Node i is a *root node* if it can reached from any other vertex by traversing a directed path. If there exists a root node then $\mathcal{G}_N$ is said to have a *spanning tree*. Let $\mathcal{B} = \text{diag}\{b_1, \ldots, b_n\}$, with $b_i = \sum_{j=1}^{N} \alpha_{ij}$, $\forall\, i \in \mathcal{V}$, the *Laplacian matrix* of $\mathcal{G}_N$ is $\mathcal{L} = \mathcal{B} - \mathcal{A}$. Since by construction $\mathcal{L}1_N = 0_N$, then 1_N is an eigenvector of $\mathcal{L}$ associated with a 0 eigenvalue. If $(i,j) \in \mathcal{E} \implies (j,i) \in \mathcal{E}$, $\mathcal{G}_N$ is *undirected*, and it results that $\mathcal{L} = \mathcal{L}^\intercal$. An undirected graph is *connected* if it has not disconnected nodes.

Proposition 1. *(In [38]) If $\mathcal{G}_N$ has a directed spanning-tree then its Laplacian matrix $\mathcal{L}$ satisfies: (a)* rank$\{\mathcal{L}\}$ *is equal to $N-1$; (b) The rest $N-1$ eigenvalues all have positive real part. In particular, if $\mathcal{G}_N$ is undirected and connected, then they are all positive and real.*

Appendix B. Stability of Time-Delay Systems

Theorem 2. *(Lyapunov-Krasovskii Stability Theorem [34]) Consider the retarded system*

$$\begin{gathered} \dot{x} = f(t, x_t), \text{ with } f : \mathbb{R}_{\geq t_0} \times \mathcal{C}([-h, 0], \mathbb{R}^n) \mapsto \mathbb{R}^n \\ x(t_0 + \theta) = \phi(\theta),\ \theta \in [-h, 0] \end{gathered} \tag{A1}$$

where $h > 0$ is the delay, $\phi \in \mathcal{C}([-h,0], \mathbb{R}^n)$ the initial condition, $x_t(\theta) = x(t+\theta) : x_t \in \mathcal{C}([-h,0], \mathbb{R}^n)$. If there exist continuous non-decreasing functions u, v, w, such that $u(\theta) > 0$ $v(\theta) > 0\ \forall\, \theta > 0$, and $u(0) = v(0) = 0$. Let there exists a continuous differentiable functional $V(t, \phi) : \mathbb{R} \times \mathcal{C}([-h,0], \mathbb{R}^n) \mapsto \mathbb{R}$ such that

$$u(\|\phi(0)\|) \leq V(t, \phi) \leq v\Big(\|\phi\|_{\mathcal{C}([-h,0], \mathbb{R}^n)}\Big) \tag{A2}$$

$$\dot{V}(t, \phi) \leq -w(\|\phi(0)\|) \tag{A3}$$

then the trivial solution of (A1) *is uniformly stable. If additionally $w(\theta) > 0$ for $\theta > 0$,* (A1) *is uniformly asymptotically stable. Moreover, if $\lim_{\theta \to \infty} u(\theta) = +\infty$,* (A1) *is globally uniformly asymptotically stable.*

Appendix C. Proof of Lemma 1

Since node 0 is a root node over the graph $\mathcal{G}_{N+1}$, from Proposition 1, its corresponding Laplacian matrix

$$\mathcal{L}_{N+1} = \left(\begin{array}{c|c} 0 & 0_N^\intercal \\ \hline b & C \end{array}\right), \tag{A4}$$

has a simple 0 eigenvalue, whereas the rest $N-1$ have all positive real part, where $b = [b_1, \ldots, b_N]^\intercal \in \mathbb{R}^N$ is such that rank$\{[b, C]\} = N$, with $b_i = 1$ if $(i,0) \in \mathcal{E}_{N+1}$, 0 otherwise. Let us now define $F = [f_{ij}] = B + \mathcal{L}$, with $B = \text{diag}\{b\} \in \mathbb{R}^{N \times N}$, and $\mathcal{L}$ is the Laplacian matrix associated with the reduced graph $\mathcal{G}_N(\mathcal{V}, \mathcal{E}_N)$. It is easy note that F is diagonally dominant, namely $|f_{ii}| \geq \sum_{j \neq i} f_{ij}\ \forall\, i$, and symmetric. Thus, the eigenvalues of F are real and non-negative. Let us now define $x = 1_N x_0$, with $x_0 \in \mathbb{R}$ and note that the following continued equality holds

$$\mathcal{L}x = 0 \quad \Longrightarrow \quad Bx + \mathcal{L}x = B1_N x_0 \quad \Longrightarrow \quad Fx = B1_N x0 \quad \Longrightarrow \quad \exists\ \ F^{-1}. \tag{A5}$$

Thus, because of F is invertible, we can conclude that $-F$ is Hurwitz. Let us now consider the matrices $A_l(k)$, and $\hat{A}_g(k)$ in (1), and matrix $\Phi(k)$ in (2). By inspection it results that

$$\Phi(k) = I_N \otimes A + \sum_{l=1}^{q} A_l(k) + \sum_{g=1}^{m} \hat{A}_g(k) \equiv I_N \otimes A - kF \otimes \bar{B} \quad \text{with} \quad A = \begin{pmatrix} 0 & 1 \\ 0 & 0 \end{pmatrix},\ \bar{B} = \begin{pmatrix} 0 & 0 \\ 1 & 2 \end{pmatrix}. \tag{A6}$$

Let D be the matrix which contains the generalized eigenvectors of F as columns, it results that

$$J_F = D^{-1}FD = \begin{pmatrix} \lambda_1 & & \\ & \ddots & \\ & & \lambda_N \end{pmatrix} \tag{A7}$$

where $\lambda_i > 0$. Let us now note that the Jordan Canonical representation associated with matrix (A6) satisfies

$$J_\Phi = \left(D^{-1} \otimes I_2\right)\Phi(D \otimes I_2) = I_N \otimes A - kD^{-1}FD \otimes \bar{B} = \begin{pmatrix} A - k\lambda_1\bar{B} & & \\ & \ddots & \\ & & A - k\lambda_N\bar{B} \end{pmatrix}. \tag{A8}$$

Consider, now the eigenpolynomial of Φ, we have

$$\det\{\Phi(k) - sI_2\} = \det\{D^{-1} \otimes I_2\}\det\{J_\Phi - sI_{2N}\}\det\{D \otimes I_2\} = \prod_{i=1}^{N}\left(s^2 + k\lambda_i s + 2k\lambda_i\right). \tag{A9}$$

From (A9), we can immediately conclude that the eigenvalues of $\Phi(k)$ will be strictly negative for all λ_i, and $k > 0$. This conclude the proof of Lemma 1.

Appendix D. Proof of Theorem 1

Let us consider the sliding manifold (36), provided below for the clarities' sake

$$s_i(t) = \dot{v}_{odi}(t) + v_{odi}(t) - z_i(t). \tag{A10}$$

By substituting the proposed voltage secondary control (35)–(38) into the DG's voltage dynamics (31), one has

$$\begin{bmatrix} \dot{v}_{odi}(t) \\ \ddot{v}_{odi}(t) \end{bmatrix} = A\begin{bmatrix} v_{odi}(t) \\ \dot{v}_{odi}(t) \end{bmatrix} + \begin{bmatrix} 0 \\ \dot{u}_i(t) + \dot{s}_i(t) \end{bmatrix} \tag{A11}$$

$$\dot{s}_i(t) = \dot{w}_i(t) - m_i \cdot \text{sign}(s_i(t)). \tag{A12}$$

For the discontinuous differential Equations (A11) and (A12), their solutions can be understood in the Filippov sense. Namely, as the solution of an appropriate differential inclusion, the existence of which is guaranteed and for which its absolute continuity is in force. The reader is referred to [22] for a comprehensive account of the necessary notions of non-smooth analysis. Particularly, following Theorem 3 in [22], namely by differentiating the locally Lipschitz Lyapunov functional $V = \sum_{i=1}^{N}|s_i(t)|$, it results that, except for Lebesgue measure zero points, which can be disregarded, it yields

$$\dot{V} \leq \quad -\min_{i\in\mathcal{V}}\{m_i - W_i\} < 0, \quad \forall\, t \geq 0. \tag{A13}$$

Thus, thanks to (33), and $m_i > \Gamma_i^P$, it results that condition $s_i = \dot{s}_i = 0$ is time-invariant for all $t \geq 0$. By substituting $u_i(t)$ in (38), and $s_i = \dot{s}_i = 0$, into (A13), the following secondo-order closed-loop local dynamic takes place

$$\begin{bmatrix} \dot{v}_{odi} \\ \ddot{v}_{odi} \end{bmatrix} = A \cdot \begin{bmatrix} v_{odi} \\ \dot{v}_{odi} \end{bmatrix} - kB\sum_{j=0}^{N}\alpha_{ij}\begin{bmatrix} 1 & 2 \end{bmatrix}\begin{bmatrix} v_{odi}(t - \tau_{ij}(t)) - v_{odj}(t - \tau_{ij}(t)) \\ \dot{v}_{odi}(t - \tau_{ij}(t)) - \dot{v}_{odj}(t - \tau_{ij}(t)) \end{bmatrix}. \tag{A14}$$

The point now is to find which conditions (A14) have to meet to asymptotically achieve the control objective (34). Let us first define the following voltage restoration error vector

$$e(t) = \left(e_1(t), \quad e_2(t), \quad \ldots, e_N(t)\right)^\intercal \quad \text{with} \quad e_i(t) = \begin{bmatrix} v_{odi}(t) - v_0 \\ \dot{v}_{odi}(t) - \dot{v}_0 \end{bmatrix} \tag{A15}$$

Consider now (1), by differentiating $e_i(t)$, after some algebraic manipulations, one derives

$$\dot{e}_i(t) = A \cdot e(t) - \alpha_{i0} k\bar{B} \cdot e_i(t - \tau_{i0}(t)) + \sum_{j=1}^{N} \alpha_{ij} k\bar{B} \cdot \left[e_i(t - \tau_{ij}(t)) - e_j(t - \tau_{ij}(t))\right]. \quad \text{(A16)}$$

Now, in order to provide a compact state-space representation of the networked error dynamics associated with the vectors (A15), and accordingly with the notation introduced for the delays in (41) and (42), where $q = \text{card}\{\mathcal{T}(t)\}$ and $m = \text{card}\{\mathcal{S}(t)\}$, it results

$$\dot{e}(t) = A_0 e(t) + \sum_{l=1}^{q} A_l e(t - \tau_l(t)) + \sum_{g=1}^{m} \hat{A}_g e(t - \sigma_g(t)). \quad \text{(A17)}$$

For stability analysis purposes, and on the basis of the so-called Leibniz-Newton formula we introduce the following transformations

$$e(t - \tau(t)) = e(t) - \int_{t-\tau(t)}^{t} \dot{e}(s) ds. \quad \text{(A18)}$$

Hence, from (A18), the networked closed-loop dynamic in (A17) can be recast as next

$$\dot{e}(t) = \Phi e(t) - \sum_{l=1}^{q} A_l \int_{t-\tau_l(t)}^{t} \dot{e}(s) ds - \sum_{g=1}^{m} \hat{A}_g \int_{t-\sigma_g(t)}^{t} \dot{e}(s) ds, \quad \text{(A19)}$$

where $\Phi = A_0 + \sum_{l=1}^{q} A_l + \sum_{g=1}^{m} \hat{A}_g$ is, by Lemma 1, Hurwitz. Now, consider the following Lyapunov-Krasovskii functional

$$\begin{aligned} \overline{V}(t) =& e(t)^{\intercal} P e(t) + \sum_{l=1}^{q} \int_{t-\tau_l(t)}^{t} e(s)^{\intercal} Q_l e(s) ds + \sum_{g=1}^{m} \int_{t-\sigma_g(t)}^{t} e(s)^{\intercal} Q_g e(s) ds \\ &+ \eta \sum_{l=1}^{q} \int_{-\tau_l^\star}^{0} \int_{t+\theta}^{t} \dot{e}(s)^{\intercal} W_l \dot{e}(s) ds d\theta + \eta \sum_{g=1}^{m} \int_{-\sigma_g^\star}^{0} \int_{t+\theta}^{t} \dot{e}(s)^{\intercal} W_g \dot{e}(s) ds d\theta, \end{aligned} \quad \text{(A20)}$$

where P, Q_l, Q_g, W_l, $W_g \in \mathbb{R}^{2N \times 2N}$ are constant, symmetric, and positive definite matrices to be determined and η is a positive scalar. Let $\tau = \max_{l,g}\{\tau_l^\star, \quad \sigma_g^\star\} > 0$, and let

$$\alpha(e(t)) = e(t)^{\intercal} P e(t), \quad \text{(A21)}$$

$$\begin{aligned} \beta(e(t)) =& e(t)^{\intercal} P e(t) + \sum_{l=1}^{q} \int_{t-\hat{\tau}}^{t} e(s)^{\intercal} Q_l e(s) ds + \sum_{g=1}^{m} \int_{t-\hat{\tau}}^{t} e(s)^{\intercal} Q_g e(s) ds \\ &+ \eta \sum_{l=1}^{q} \int_{-\hat{\tau}}^{0} \int_{t+\theta}^{t} \dot{e}(s)^{\intercal} W_l \dot{e}(s) ds d\theta + \eta \sum_{g=1}^{m} \int_{-\hat{\tau}}^{0} \int_{t+\theta}^{t} \dot{e}(s)^{\intercal} W_g \dot{e}(s) ds d\theta, \end{aligned} \quad \text{(A22)}$$

then, it results that $\overline{V}$ in (A20) mets the requirements of Theorem 2 in Appendix B, namely,

$$\alpha(e(t)) \leq \overline{V}(t) \leq \beta(e(t - \hat{\tau})). \quad \text{(A23)}$$

Now, differentiating (A20) along the trajectories of (A19), it follows that

$$\begin{aligned}\dot{\bar{V}}(t) = \; & e(t)^{\intercal}(\Phi^{\intercal}P + P\Phi)e(t) - 2e(t)^{\intercal}P\sum_{l=1}^{q} A_l \int_{t-\tau_l(t)}^{t} \dot{e}(s)ds - 2e(t)^{\intercal}P\sum_{g=1}^{m} \hat{A}_g \int_{t-\sigma_g(t)}^{t} \dot{e}(s)ds \\ & + e(t)^{\intercal}\sum_{l=1}^{q} Q_l e(t) - \sum_{l=1}^{q} e(t-\tau_l(t))^{\intercal}Q_l e(t-\tau_l(t))(1-\dot{\tau}_l(t)) \\ & + e(t)^{\intercal}\sum_{g=1}^{m} Q_g e(t) - \sum_{g=1}^{m} e(t-\sigma_g(t))^{\intercal}Q_g e(t-\sigma_g(t))(1-\dot{\sigma}_g(t)) \\ & + \eta\dot{e}(t)^{\intercal}\sum_{l=1}^{q} \tau_l^{\star}W_l\dot{e}(t) - \eta\sum_{l=1}^{q}\int_{t-\tau_l^{\star}}^{t} \dot{e}(s)^{\intercal}W_l\dot{e}(s)ds \\ & + \eta\dot{e}(t)^{\intercal}\sum_{g=1}^{m} \sigma_g^{\star}W_g\dot{e}(t) - \eta\sum_{g=1}^{m}\int_{t-\sigma_g^{\star}}^{t} \dot{e}(s)^{\intercal}W_g\dot{e}(s)ds \end{aligned} \tag{A24}$$

Because of Assumption 2, and by adding to the right-hand side of (A24) the next identically zero quantity

$$\sum_{g=1}^{m} \sigma_g^{\star}e(t)^{\intercal}R_g e(t) - \sum_{g=1}^{m} \sigma_g^{\star}e(t)^{\intercal}R_g e(t) = 0,$$

where $R_g \succ 0$ is a matrix to be determined, (A24) can be upper-estimated as next

$$\begin{aligned}\dot{\bar{V}}(t) \leq & e(t)^{\intercal}\left(\Phi^{\intercal}P + P\Phi + \sum_{l=1}^{q} Q_l + \sum_{g=1}^{m} Q_g + \sum_{g=1}^{m} \sigma_g^{\star}R_g\right)e(t) - 2e(t)^{\intercal}P\sum_{l=1}^{q} A_l \int_{t-\tau_l(t)}^{t} \dot{e}(s)ds \\ & - 2e(t)^{\intercal}P\sum_{g=1}^{m} \hat{A}_g \int_{t-\sigma_g(t)}^{t} \dot{e}(s)ds - \sum_{l=1}^{q} e(t-\tau_l(t))^{\intercal}Q_l e(t-\tau_l(t))(1-d_l) \\ & - \sum_{g=1}^{m} e(t-\sigma_g(t))^{\intercal}Q_g e(t-\sigma_g(t))(1-d_g) + \eta\dot{e}(t)^{\intercal}\left(\sum_{l=1}^{q} \tau_l^{\star}W_l + \sum_{g=1}^{m} \sigma_g^{\star}W_g\right)\dot{e}(t) \\ & - \eta\sum_{l=1}^{q}\int_{t-\tau_l^{\star}}^{t} \dot{e}(s)^{\intercal}W_l\dot{e}(s)ds - \eta\sum_{g=1}^{m}\int_{t-\sigma_g^{\star}}^{t} \dot{e}(s)^{\intercal}W_g\dot{e}(s)ds - e(t)^{\intercal}\sum_{g=1}^{m} \sigma_g^{\star}R_g e(t) \end{aligned} \tag{A25}$$

Let us now introduce the following matrix

$$H = \sum_{g=1}^{m} \sigma_g^{\star}W_g + \sum_{l=1}^{q} \tau_l^{\star}W_l \tag{A26}$$

and, as in [26], the following state vector

$$\rho(t) = \left(e(t)^{\intercal}, \; \int_{t-\tau_l^{\star}}^{t} \dot{e}(s)^{\intercal}ds, \; \int_{t-\sigma_g^{\star}}^{t} \dot{e}(s)^{\intercal}ds\right)^{\intercal} \in \mathbb{R}^{6N}. \tag{A27}$$

Now, by applying the Jensen inequality (7) on the following integral terms

$$\begin{aligned} -\eta\sum_{l=1}^{q}\int_{t-\tau_l^{\star}}^{t} \dot{e}(s)^{\intercal}W_l\dot{e}(s)ds \leq & -\frac{\eta}{\tau_l^{\star}}\left(\int_{t-\tau_l^{\star}}^{t} \dot{e}(s)ds\right)^{\intercal}\sum_{l=1}^{q} W_l\left(\int_{t-\tau_l^{\star}}^{t} \dot{e}(s)ds\right), \\ -\eta\sum_{g=1}^{m}\int_{t-\sigma_g^{\star}}^{t} \dot{e}(s)^{\intercal}W_g\dot{e}(s)ds \leq & -\frac{\eta}{\sigma_g^{\star}}\left(\int_{t-\sigma_g^{\star}}^{t} \dot{e}(s)ds\right)^{\intercal}\sum_{g=1}^{m} W_g\left(\int_{t-\sigma_g^{\star}}^{t} \dot{e}(s)ds\right), \end{aligned} \tag{A28}$$

and after substituting (A26), and (A28), the inequality (A25) can further be upper-estimated as follows

$$\begin{aligned}\dot{\bar{V}}(t) \leq & \rho(t)^{\intercal}\Sigma\rho(t) + \eta\dot{e}(t)^{\intercal}H\dot{e}(t) - \sum_{l=1}^{q} e(t-\tau_l(t))^{\intercal}Q_l e(t-\tau_l(t))(1-d_l) \\ & - e(t)^{\intercal}\sum_{g=1}^{m}\sigma_g^{\star}R_g e(t) - \sum_{g=1}^{m} e(t-\sigma_g(t))^{\intercal}Q_g e(t-\sigma_g(t))(1-d_g) \end{aligned} \tag{A29}$$

where

$$\Sigma = \begin{pmatrix} \Phi^{\intercal}P + P\Phi + \sum_{l=1}^{q}Q_l + \sum_{g=1}^{m}\left(Q_g + \sigma_g^{\star}R_g\right) & -2P\sum_{l=1}^{q}A_l & -2P\sum_{g=1}^{m}\hat{A}_g \\ & -\frac{\eta}{\tau_l^{\star}}\sum_{l=1}^{q}W_l & 0_{2N\times 2N} \\ 0 & & -\frac{\eta}{\sigma_g^{\star}}\sum_{g=1}^{m}W_g \end{pmatrix}. \tag{A30}$$

Define now the following augmented state vector

$$\xi(t) = \left[e(t)^{\intercal},\ e(t-\tau_1(t))^{\intercal},\ \ldots,\ e(t-\tau_q(t))^{\intercal},\ e(t-\sigma_1(t))^{\intercal},\ldots,\ e(t-\sigma_m(t))^{\intercal}\right]^{\intercal}, \tag{A31}$$

then, by substituting (A17) into the second term of (A29), and after lengthy manipulations, (A29) can finally be recast as next

$$\dot{\bar{V}}(t) \leq \rho(t)^{\intercal}\Sigma\rho(t) + \eta\xi(t)^{\intercal}\Theta\xi(t), \tag{A32}$$

where Θ is an upper triangular block matrix in the from

$$\Theta = \begin{pmatrix} \Theta_{1,1} & 2A_0^{\intercal}HA_1 & \ldots & \ldots & 2A_0^{\intercal}HA_q & 2A_0^{\intercal}H\hat{A}_1 & \ldots & 2A_0^{\intercal}H\hat{A}_m \\ & \Theta_{2,2} & 2A_1^{\intercal}HA_2 & \ldots & 2A_1^{\intercal}HA_q & 2A_1^{\intercal}H\hat{A}_1 & \ldots & 2A_1^{\intercal}H\hat{A}_m \\ & & \ddots & \ddots & \ldots & \ldots & \ldots & \vdots \\ & & & \ddots & 2A_q^{\intercal}H\hat{A}_1 & \ldots & \ldots & \vdots \\ & & & & \Theta_{q+1,q+1} & 2\hat{A}_1^{\intercal}H\hat{A}_2 & \vdots & \vdots \\ & & & & & \Theta_{q+2,q+2} & \ddots & \vdots \\ & & & & & & \ddots & 2\hat{A}_{m-1}^{\intercal}H\hat{A}_m \\ & & & & & & & \Theta_{q+m+1,q+m+1} \end{pmatrix} \tag{A33}$$

and which diagonal blocks take the following form

$$\begin{aligned} \Theta_{(1,1)} &= -\frac{1}{\eta}\sum_{g=1}^{m}\sigma_g^{\star}R_g + A_0^{\intercal}HA_0, \\ \Theta_{(1+l,1+l)} &= -\frac{(1-d_l)}{\eta}Q_l + A_l^{\intercal}HA_l, \quad l = 1,2,\ldots,q, \\ \Theta_{(1+q+g,1+q+g)} &= -\frac{(1-d_g)}{\eta}Q_g + \hat{A}_g^{\intercal}H\hat{A}_g, \quad g = 1,2,\ldots,m. \end{aligned} \tag{A34}$$

Hence, if the LMIs (3)–(6) are satisfied, then the matrices Σ in (A30) and Θ in (A33) are negative definite. Therefore, it results that $\dot{V}(t) < 0$ and thus also condition (A3) of Theorem 2 is satisfied. Moreover, by choosing $\alpha(s)$ as in (A21), it follows that $\lim_{s\to\infty}\alpha(s) = +\infty$, and hence the error vector $e(t)$ globally uniformly converges to zero, which it further implies the voltage restoration achievement. This concludes the proof.

References

1. Guerrero, J.M.; Vasquez, J.C.; Matas, J.; De Vicuña, L.G.; Castilla, M. Hierarchical control of droop-controlled AC and DC microgrids—A general approach toward standardization. *IEEE Trans. Ind. Electron.* **2011**, *58*, 158–172. [CrossRef]
2. Simpson-Porco, J.W.; Dörfler, F.; Bullo, F. Synchronization and power sharing for droop-controlled inverters in islanded microgrids. *Automatica* **2013**, *49*, 2603–2611. [CrossRef]
3. D'silva, S.; Shadmand, M.; Bayhan, S.; Abu-Rub, H. Towards Grid of Microgrids: Seamless Transition between Grid-Connected and Islanded Modes of Operation. *IEEE Open J. Ind. Electron. Soc.* **2020**, *1*, 66–81. [CrossRef]
4. Lopes, J.P.; Moreira, C.; Madureira, A. Defining control strategies for microgrids islanded operation. *IEEE Trans. Power Syst.* **2006**, *21*, 916–924. [CrossRef]
5. Dörfler, F.; Simpson-Porco, J.W.; Bullo, F. Breaking the hierarchy: Distributed control and economic optimality in microgrids. *IEEE Trans. Control Netw. Syst.* **2016**, *3*, 241–253. [CrossRef]
6. Shafiee, Q.; Guerrero, J.M.; Vasquez, J.C. Distributed secondary control for islanded microgrids—A novel approach. *IEEE Trans. Power Syst.* **2014**, *29*, 1018–1031. [CrossRef]
7. Simpson-Porco, J.W.; Dörfler, F.; Bullo, F. Voltage stabilization in microgrids via quadratic droop control. *IEEE Trans. Autom. Control* **2017**, *62*, 1239–1253. [CrossRef]
8. Guo, F.; Wen, C.; Mao, J.S.Y. Distributed secondary voltage and frequency restoration control of droop-controlled inverter-based microgrids. *IEEE Trans. Ind. Electron.* **2015**, *62*, 4355–4364. [CrossRef]
9. Bidram, A.; Davoudi, A.; Lewis, F.L.; Ge, S.S. Distributed adaptive voltage control of inverter-based microgrids. *IEEE Trans. Energy Convers.* **2014**, *29*, 862–872. [CrossRef]
10. Bidram, A.; Davoudi, A.; Lewis, F.L.; Qu, Z. Secondary control of microgrids based on distributed cooperative control of multi-agent systems. *IET Gen. Trans. Distrib.* **2013**, *7*, 822–831. [CrossRef]
11. Pilloni, A.; Pisano, A.; Usai, E. Robust Finite-Time Frequency and Voltage Restoration of Inverter-Based Microgrids via Sliding-Mode Cooperative Control. *IEEE Trans. Ind. Electron.* **2018**, *65*, 907–917. [CrossRef]
12. Xu, Y.; Guo, Q.; Sun, H.; Fei, Z. Distributed discrete robust secondary cooperative control for islanded microgrids. *IEEE Trans. Smart Grid* **2019**, *10*, 3620–3629. [CrossRef]
13. Zhang, M.; Li, Y.; Liu, F.; Lee, W.J.; Peng, Y.; Liu, Y.; Li, W.; Cao, Y. A robust distributed secondary voltage control method for islanded microgrids. *Int. J. Electr. Power Energy Syst.* **2020**, *121*, 105938. [CrossRef]
14. Liu, S.; Wang, X.; Liu, P.X. Impact of Communication Delays on Secondary Frequency Control in an Islanded Microgrid. *IEEE Trans. Ind. Electron.* **2015**, *62*, 2021–2031. [CrossRef]
15. Lai, J.; Zhou, H.; Lu, X.; Yu, X.; Hu, W. Droop-based distributed cooperative control for microgrids with time-varying delays. *IEEE Trans. Smart Grid* **2016**, *7*, 1775–1789. [CrossRef]
16. Xie, Y.; Lin, Z. Distributed Event-Triggered Secondary Voltage Control for Microgrids With Time Delay. *IEEE Trans. Syst. Man Cybern. Syst.* **2019**, *49*, 1582–1591. [CrossRef]
17. Jingang, L.; Lu, X.; Monti, A. Distributed secondary voltage control for autonomous microgrids under additive measurement noises and time delays. *IET Gener. Transm. Distrib.* **2019**, *13*, 2976–2985.
18. Afshari, A.; Karrari, M.; Baghaee, H.R.; Gharehpetian, G.B. Resilient cooperative control of AC microgrids considering relative state-dependent noises and communication time-delays. *IET Renew. Power Gener.* **2020**, *14*, 1321–1331. [CrossRef]
19. Zhao, C.; Sun, W.; Wang, J.; Li, Q.; Mu, D.; Xu, X. Distributed Cooperative Secondary Control for Islanded Microgrid With Markov Time-Varying Delays. *IEEE Trans. Energy Conv.* **2019**, *34*, 2235–2247. [CrossRef]
20. Lou, G.; Gu, W.; Lu, X.; Xu, Y.; Hong, H. Distributed Secondary Voltage Control in Islanded Microgrids With Consideration of Communication Network and Time Delays. *IEEE Trans. Smart Grid* **2020**, *11*, 3702–3715. [CrossRef]
21. Du, Y.; Tu, H.; Yu, H.; Lukic, S. Accurate Consensus-Based Distributed Averaging With Variable Time Delay in Support of Distributed Secondary Control Algorithms. *IEEE Trans. Smart Grid* **2020**, *11*, 2918–2928. [CrossRef]
22. Pilloni, A.; Franceschelli, M.; Pisano, A.; Usai, E. Sliding mode based robustification of consensus and distributed optimization control protocols. *IEEE Trans. Autom. Control* **2020**, *99*, 1. [CrossRef]
23. Sun, Y.G.; Wang, L.; Xie, G. Average consensus in networks of dynamic agents with switching topologies and multiple time-varying delays. *Syst. Control Lett.* **2008**, *57*, 175–183. [CrossRef]
24. Petrillo, A.; Salvi, A.; Santini, S.; Valente, A.S. Adaptive synchronization of linear multi-agent systems with time-varying multiple delays. *J. Frankl. Inst.* **2017**, *354*, 8586–8605. [CrossRef]
25. Gholami, M.; Pisano, A.; Usai, E. Robust Distributed Optimal Secondary Voltage Control in Islanded Microgrids with Time-Varying Multiple Delays. In Proceedings of the 2020 IEEE 21st Workshop on Control and Modeling for Power Electronics (COMPEL), Aalborg, Denmark, 9–12 November 2020; pp. 1–8.
26. Shi, L.; Zhu, H.; Zhong, S.; Zeng, Y.; Cheng, J. Synchronization for time-varying complex networks based on control. *J. Comput. Appl. Math.* **2016**, *301*, 178–187. [CrossRef]
27. Xin, H.; Qu, Z.; Seuss, J.; Maknouninejad, A. A self-organizing strategy for power flow control of photovoltaic generators in a distribution network. *IEEE Trans. Power Syst.* **2010**, *26*, 1462–1473. [CrossRef]
28. Liu, J.; Vazquez, S.; Wu, L.; Marquez, A.; Gao, H.; Franquelo, L.G. Extended state observer-based sliding-mode control for three-phase power converters. *IEEE Trans. Ind. Electron.* **2016**, *64*, 22–31. [CrossRef]

29. Ahumada, C.; Cárdenas, R.; Saez, D.; Guerrero, J.M. Secondary control strategies for frequency restoration in islanded microgrids with consideration of communication delays. *IEEE Trans. Smart Grid* **2016**, *7*, 1430–1441. [CrossRef]
30. Bidram, A.; Davoudi, A.; Lewis, F.L.; Guerrero, J.M. Distributed cooperative secondary control of microgrids using feedback linearization. *IEEE Trans. Power Syst.* **2013**, *28*, 3462–3470. [CrossRef]
31. Pogaku, N.; Prodanovic, M.; Green, T.C. Modeling, analysis and testing of autonomous operation of an inverter-based microgrid. *IEEE Trans. Power Electron.* **2007**, *22*, 613–625. [CrossRef]
32. Pilloni, A.; Pisano, A.; Usai, E. Voltage Restoration of Islanded Microgrids via Cooperative Second-Order Sliding Mode Control. *IFAC-PapersOnLine* **2017**, *50*, 9637–9642. [CrossRef]
33. Levant, A. Higher-order sliding modes, differentiation and output-feedback control. *Int. J. Control* **2003**, *76*, 924–941. [CrossRef]
34. Gu, K.; Kharitonov, V.; Chen, J. Stability of Time-Delay Systems. In *Control Engineering*; Birkhäuser: Boston, FL, USA, 2012.
35. Fridman, E.; Orlov, Y. Exponential stability of linear distributed parameter systems with time-varying delays. *Automatica* **2009**, *45*, 194–201. [CrossRef]
36. Luo, Y.; Effenberger, F. Timestamp Provisioning in IEEE 802.3. IEEE 802 LAN/MAN Standards Committee. 2009. Available online: www.ieee802.org/3/time_adhoc/ (accessed on 15 December 2020).
37. Chen, G.; Lewis, F.L. Leader-following control for multiple inertial agents. *Int. J. Robust Nonlinear Control* **2011**, *21*, 925–942. [CrossRef]
38. Olfati-Saber, R.J.; Fax, A.; Murray, R.M. Consensus and cooperation in networked multi-agent systems. *Proc. IEEE* **2007**, *95*, 215–233. [CrossRef]